Laser-plasma physics of high energy in Lebedev

V. Yu. Bychenkov

P.N.Lebedev Physical Institute of the Russian Academy of Science

Lebedev Physics Institute, Russian Academy of Sciencies, Moscow

Asian Forum for Accelerators and Detectors (AFAD-2021),
Budker Institute of Nuclear Physics, Novosibirsk, Russia
16-18, March 2021

High Energy Laser-Plasma Physics Lab

V. Yu. Bychenkov

High Field Science

S. G. Bochkarev, A. V. Brantov, D. A. Gozhev, V. F. Kovalev, A. S. Kuratov, M. G. Lobok, I. I. Metelskii, O. E. Vais

Relativistic optics
Acceleration
Relativistic nanoplasmonics
Secondary emission
Nuclear photonics

ICF Laser-Plasma Interaction

A.V. Brantov, S. I. Glazyrin, S. A. Karpov, M. A. Rakitina

Instabilities in corona
Fast particles
Nonlocal transport
Nonlinear structures

New regime of wakefield acceleration→ Relativistic self-trapping

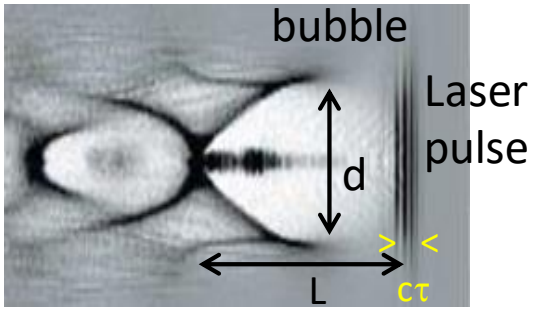

$0.004n_c$

Tajima T. and Dawson J. M. 1979 Phys. Rev. Lett. **43** 267

3D plasma wave

Pukhov A. and Meyer-ter-Vehn J., 2002 Appl. Phys. B: Lasers Opt. **74** 355

"bubble" regime

$c\tau < L \quad c\tau < d$

Quasi-monoenergetic electrons, pC charge

Up to 10 GeV (gas jet, gas capillary)

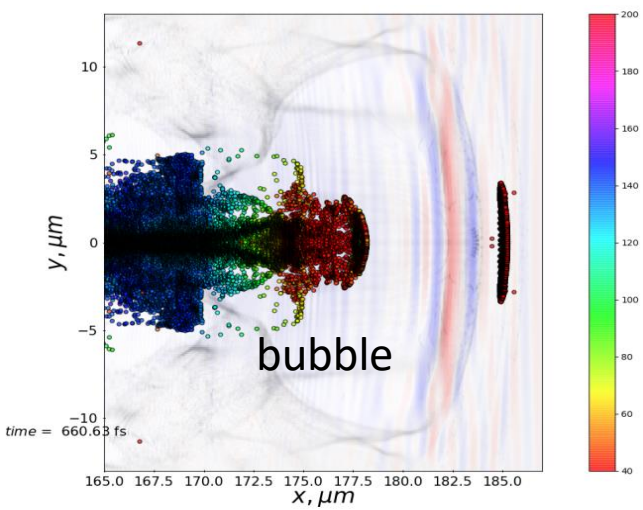

$\cancel{c\tau < L \quad c\tau < d}$

$L \approx c\tau > d$

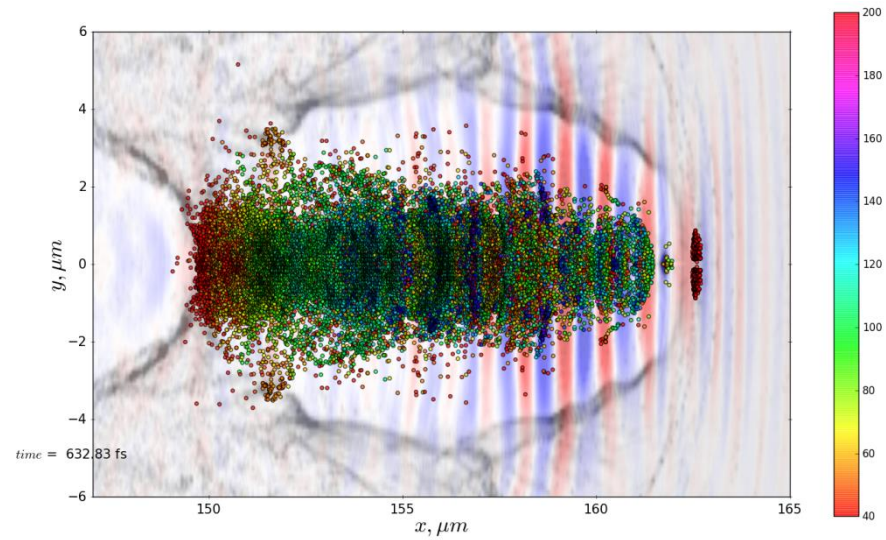

Laser bullet

Laser bullet acceleration regime

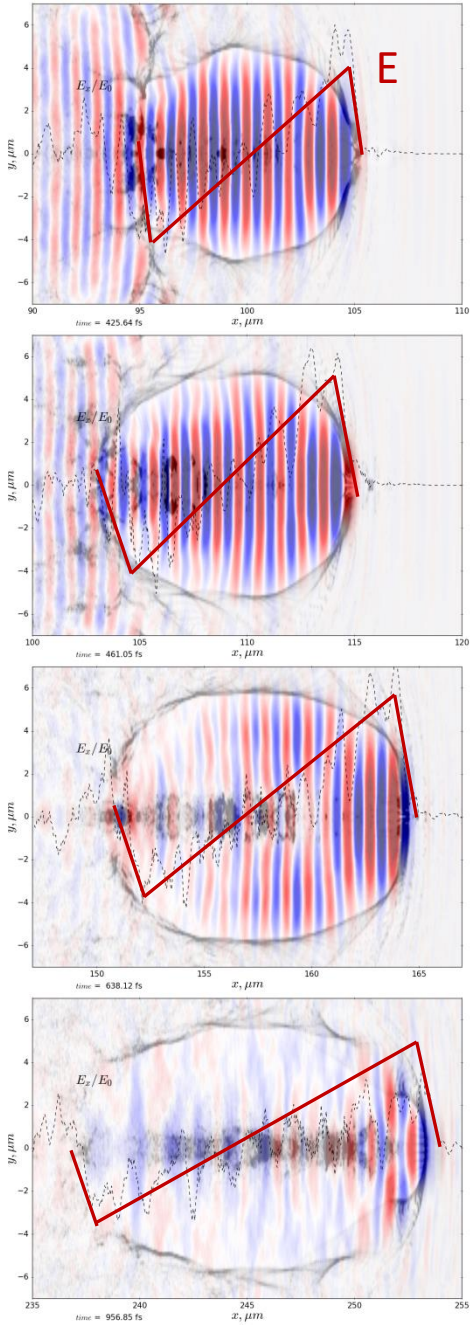

Propagation over ~ 10 Rayleigh lengths

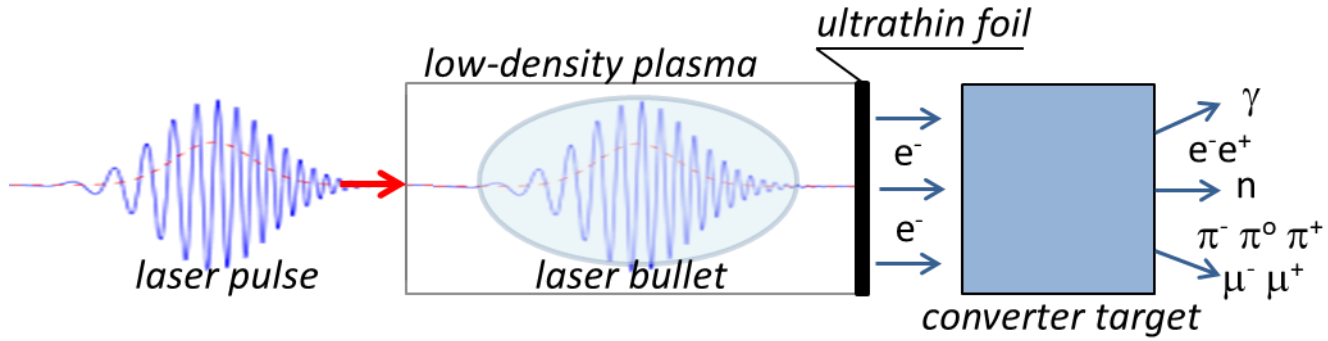

$$a_0 = 0.85\lambda[\mu m]\sqrt{I[W/cm^2]} \times 10^{-9}$$

$$R \cong \frac{c}{\omega_p}\alpha\sqrt{a_0}$$

α - numeric factor ~ (1-2)

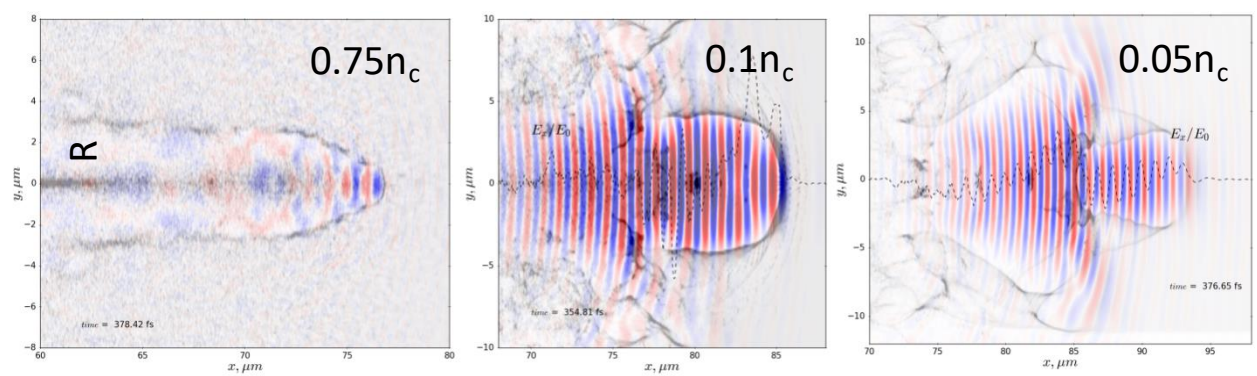

R (n, I) - matching

The matched cavern spot size condition

$$R \cong \frac{c}{\omega_p}\alpha\sqrt{a_0} \qquad R = \frac{c}{\omega}\sqrt{\frac{n_c}{n_e}}\left(\frac{16\alpha^4 P}{P_c}\right)^{1/6}$$

P – laser pulse power

1 Gordienko S and Pukhov A 2005 *Phys. Plasmas 12*, 043109 $\alpha \approx 1.12$

2 Lu M *et al* 2007 *Phys. Rev. STAB* **10**, 061301 $\alpha \approx 2$

3 Lobok M G Brantov A V Gozhev D A and Bychenkov V Yu 2018 *Plasma Phys. Control. Fusion* **60** 084010 $\alpha \approx 1.22$

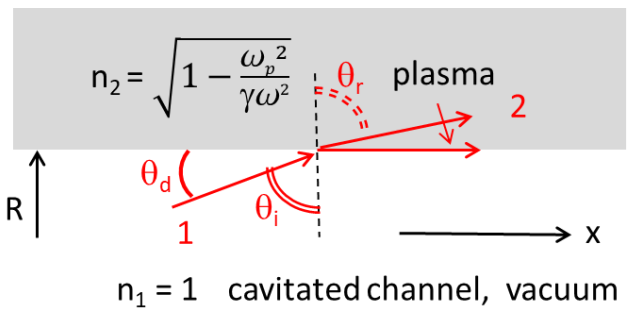

Snell's law

$$\theta_d \simeq \lambda/\pi R \qquad \theta_i = \pi/2 - \theta_d$$

$$n_1 \sin\theta_i = n_2 \sin\theta_r$$

condition of the total internal reflection, $\theta_r = \pi/2$

M.G.Lobok, A.V.Brantov, and V.Yu.Bychenkov, Phys. Plasmas **26**, 123107 (2019)

$$\theta_d^2 \simeq \left(\frac{2c}{\omega R}\right)^2 \simeq \frac{\omega_p^2}{\gamma\omega^2} \simeq \frac{\sqrt{2}\omega_p^2}{a_0\omega^2} \qquad \gamma = \sqrt{1 + a_0^2/2} \simeq a_0/\sqrt{2}$$

$$R \cong \frac{c}{\omega_p} 2^{3/4}\sqrt{a_0}$$

Theory:
V.F.Kovalev and V.Yu.Bychenkov, Phys. Rev. E **99**, 043201 (2019);
V.Yu.Bychenkov *et al.*, Plasma Phys. Contr. Fus. **61**, 124004 (2019);
V.Yu.Bychenkov and V.F.Kovalev, Radiophysics & Quantum Electronics **63**, N9 (2020)

Electron acceleration. Stochastic injection.

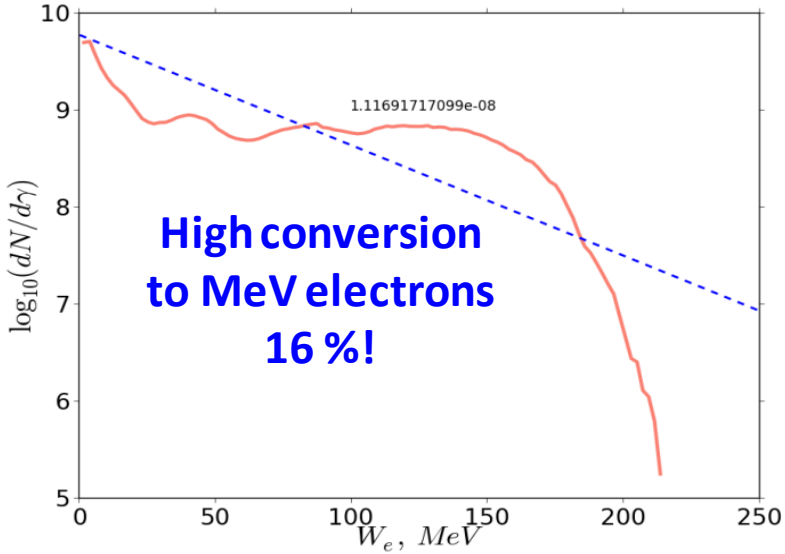

optimum target thickness:

$$l_0 = v_g c\tau_L/(c - v_g) \approx c^2\tau_L/(c - v_g)$$
$$l_{opt} \simeq l_0 \simeq l_d$$

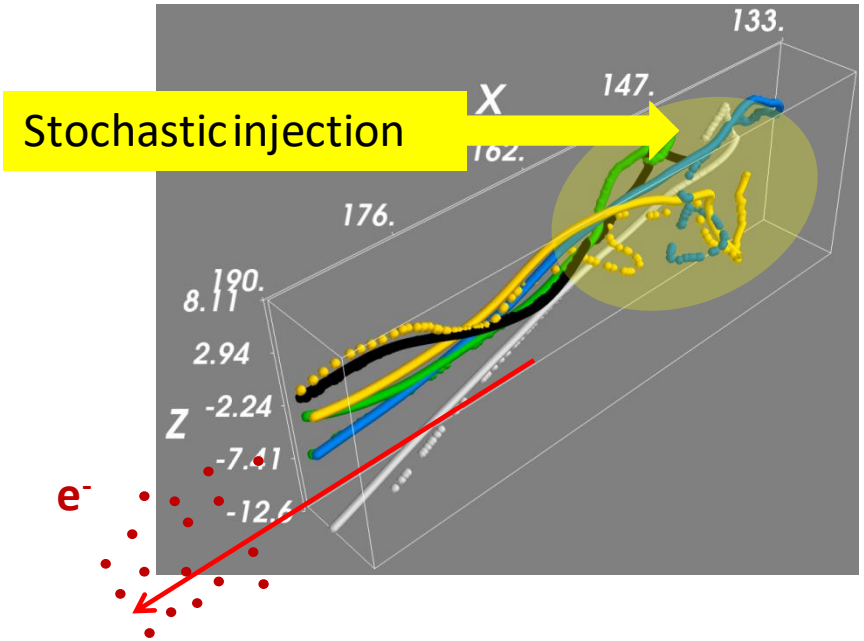

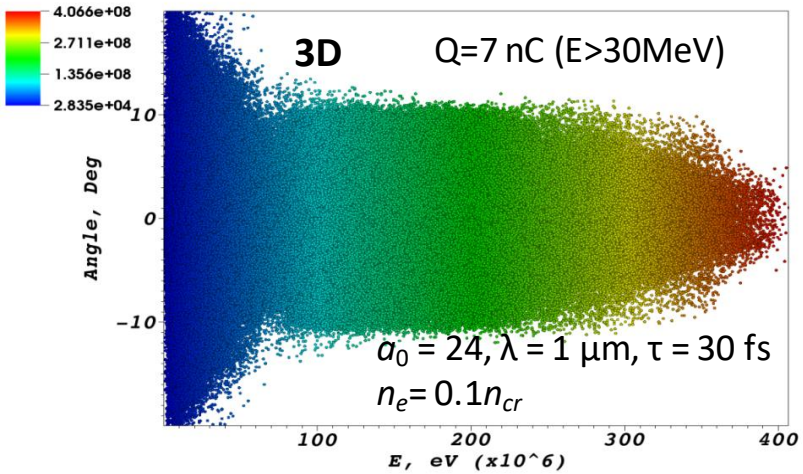

M.G.Lobok, A.V.Brantov, D.A.Gozhev, and V.Yu.Bychenkov
Plasma Phys. Contr. Fus. 60, 084010 2018

Electron conversion to gamma emission

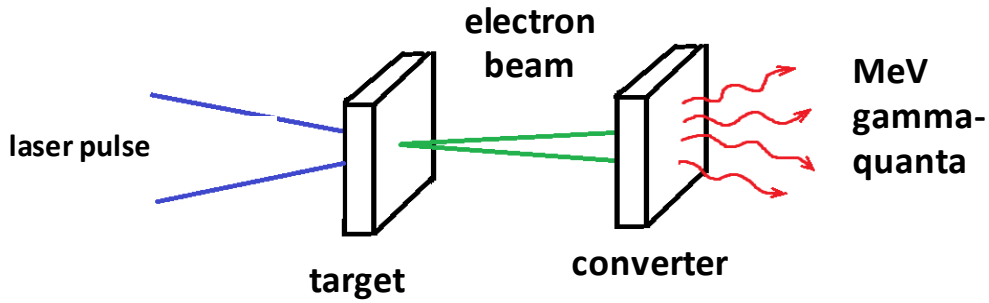

8×10^{20} W/cm^2, λ=1μm, 30fs, d=4μm, n_e=0.1n_c, Q=7nC

Deep γ-radiography
(10-20 cm dense matter)
Single shot radiography:
multi-tens of nQ

PW lasers

polar angular diagram for high-energy γ

Pt of 6 mm thickness

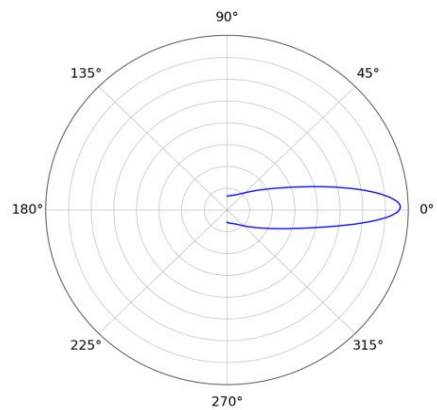

M.G.Lobok, A.V.Brantov, and V.Yu.Bychenkov, Phys. Plasmas **26**, 123107 (2019)
gammas, pairs, neutrons, pions

Angular γ distribution

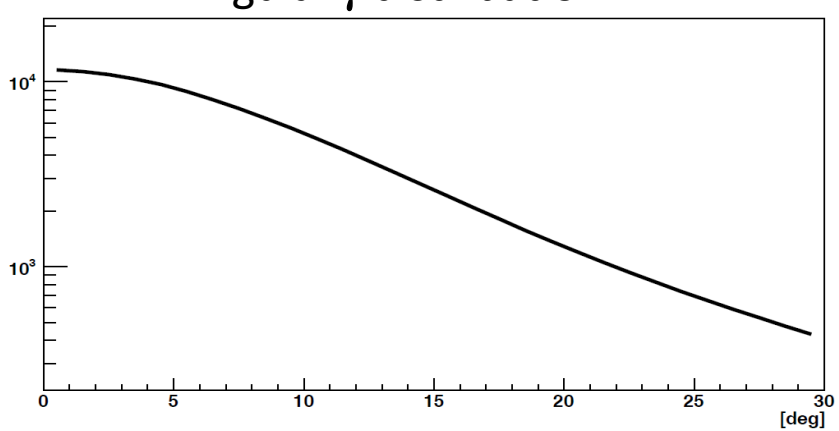

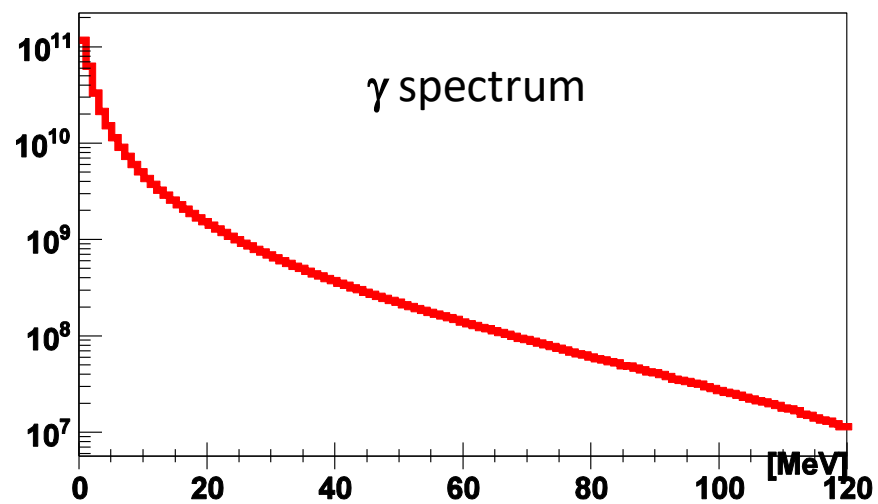

X-ray generation

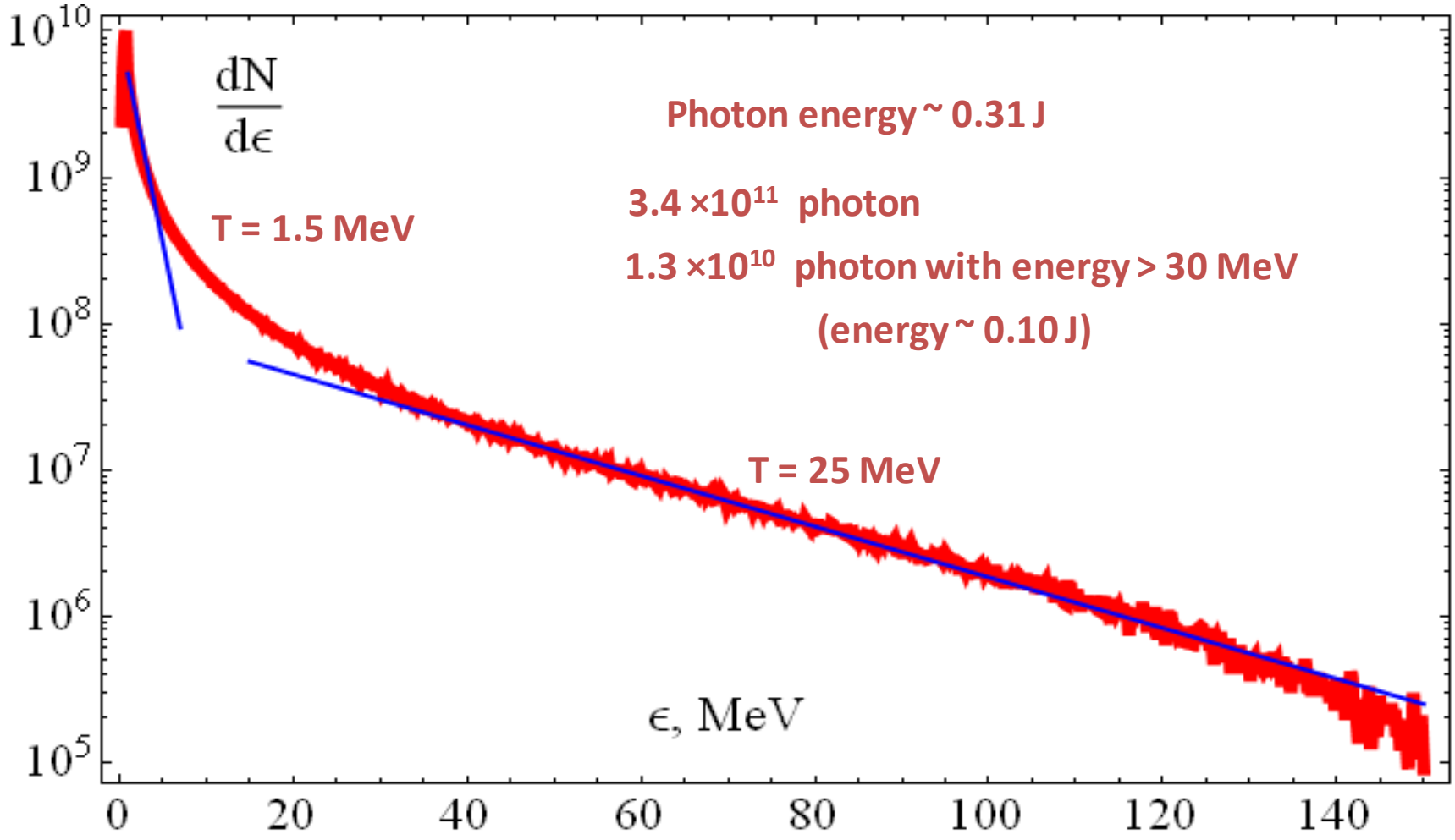

Conversion from laser to gamma-rays of ~ 7 %

Betatron emission

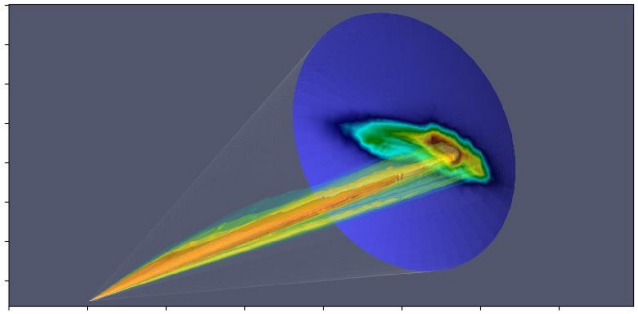

135 TW $\rightarrow 3\times10^{10}$ ph > 10 keV
1.2 PW $\rightarrow 10^{11}$ ph > 10 keV
The laser-to-gammas energy conversion efficiency ~ 10^{-4} for ~100 keV ph
and few tenths % for entire keV-range.

Angular-integrated spectra of photons emitted per single electron along the laser propagation through the target: a_0 = 24 (a) and a_0 = 72 (b).

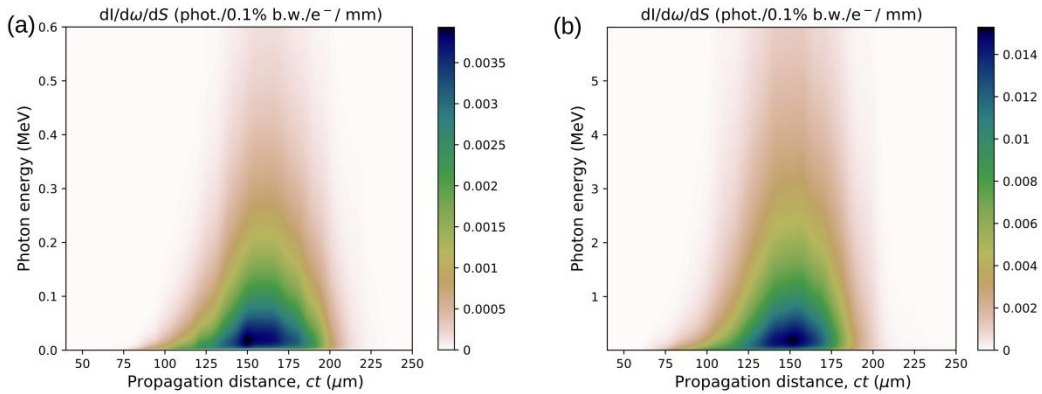

Angular-integrated photon spectra in 0.1% BW (a). The θ-distribution of the betatron radiation spectra for a_0 = 24 (b) and a_0 = 72 (c).

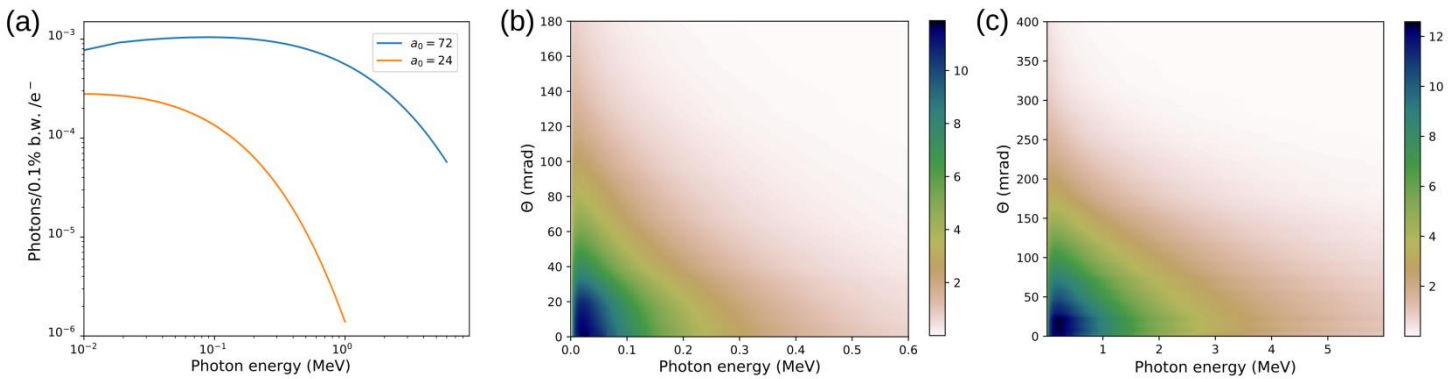

THz surface pulse generation by escaping electrons

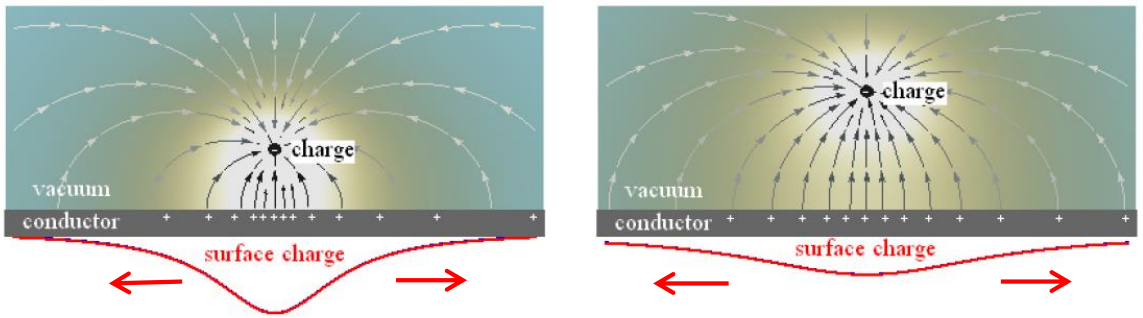

FIG. 1. Cartoon of electric field distribution and surface charge (shown by red line at the bottom) for electron line (position shown by black circle) moving with $v = 0.1c$ in vacuum from conductor boundary at two instants.

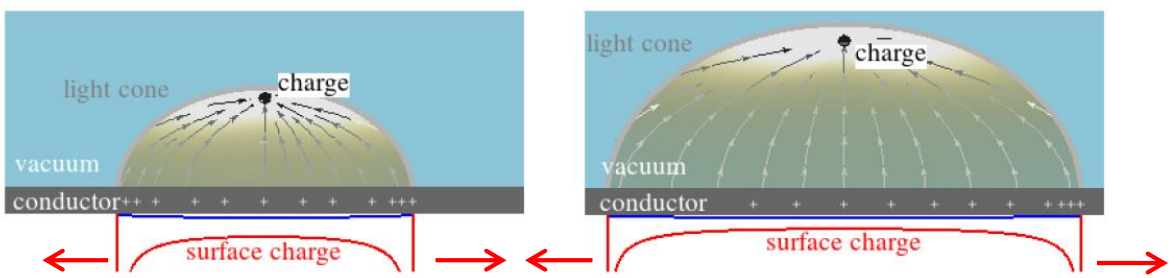

FIG. 2. Cartoon of electric field distribution and surface charge (shown by red line at the bottom) for electron line (position shown by black circle) moving with $v = 0.9c$ in vacuum from conductor boundary at two instants.

A. V. Brantov, A. S. Kuratov, Yu. M. Aliev, and V. Yu. Bychenkov, Ultrafast target charging due to polarization triggered by laser-accelerated electrons, PHYS. REV. E **102**, 021202(R) (2020)

theory, FDTP numerical modeling, PIC simulation

Generation and propagation of a transient electromagnetic pulse and a lateral current in the wave form along the target surface at the speed of light

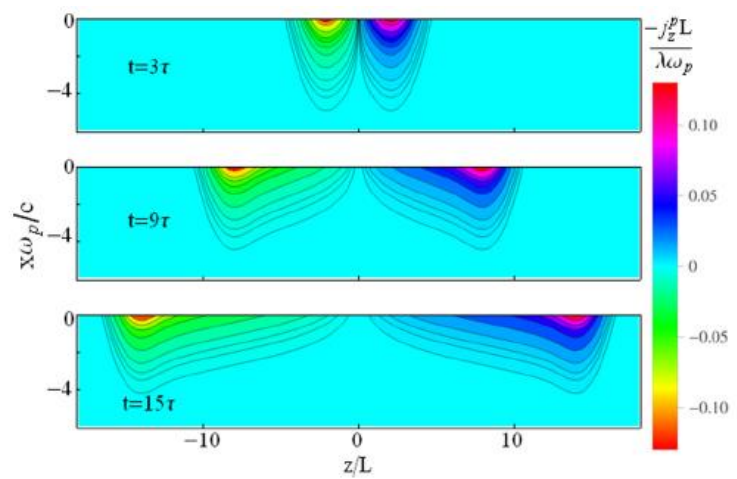

Polarization triggered current

FDTD numerical simulations

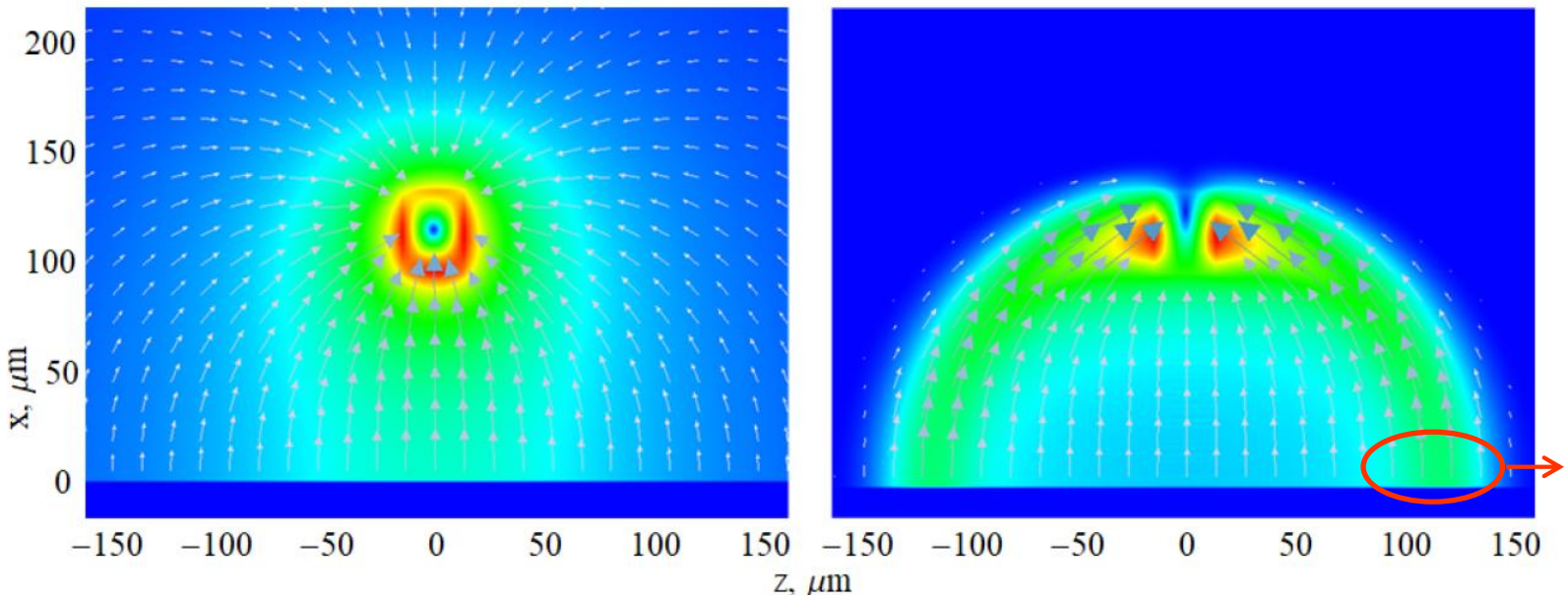

FIG. 3. Electric field distribution for electron bunch moving with $v = 0.2c$ at instant of 2.44 ps (left panel) and $v = 0.9c$ at instant of 551 fs (right panel) from FDTD modeling for $L = c\tau = 20\,\mu$m.

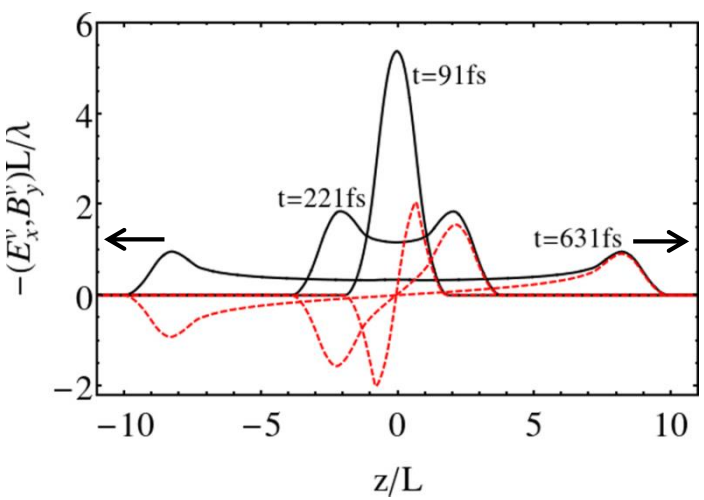

Up to TV/m fields

FIG. 4. Evolution of the vacuum electric field $E_{x0}^v(t, z)$ (black curves) and magnetic field $B_{y0}^v(t, z)$ (red dashed curves) at the target-vacuum boundary from FDTD modeling for $L = c\tau = 20\ \mu$m.

PIC simulations of surface wave

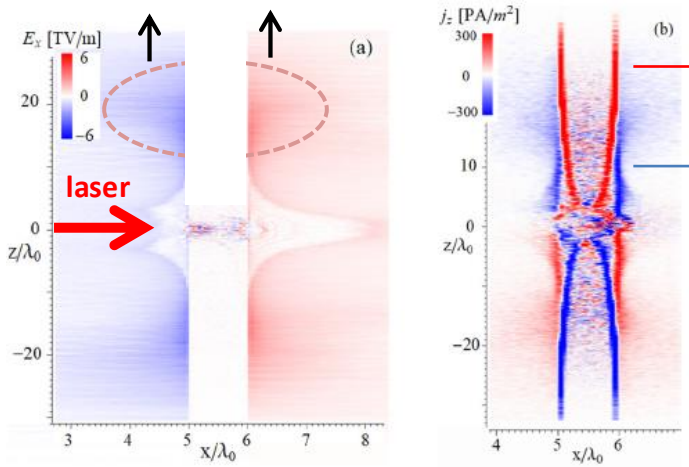

FIG. 5. Spatial distributions (from PIC simulation) of the electric field (a) and current (b) together with their cross-section profiles (along the line $z = 17\lambda_0$) (c) at $t = 190$ fs (80 fs after the laser pulse maximum arrived at the target). Evolution of the vacuum electric field at the front target surface ($x = 4.9\lambda_0$) E^f_{x0} (black curves) and back target surface ($x = 6.1\lambda_0$) E^b_{y0} (blue dashed curves) is shown in panel (d).

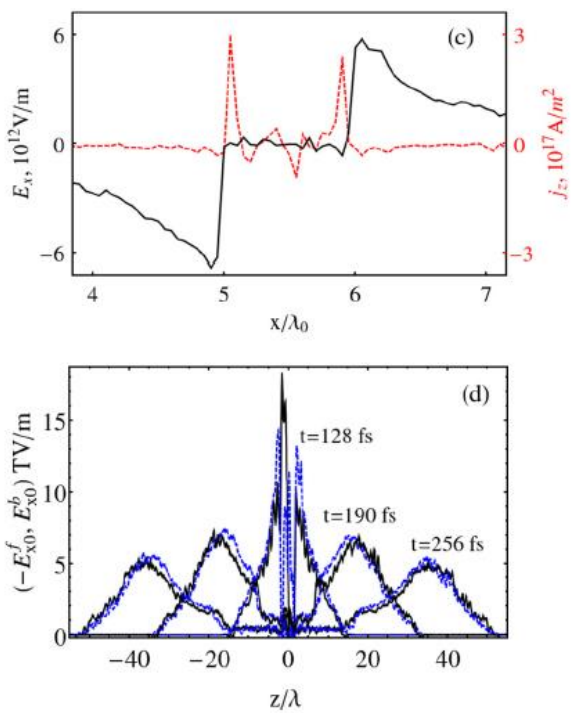

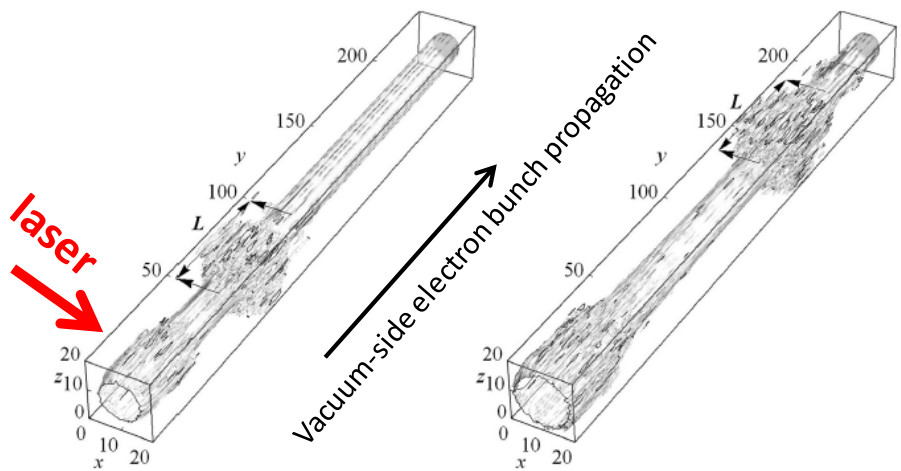

Laser triggered stochastic volumetric heating of micro-structured targets

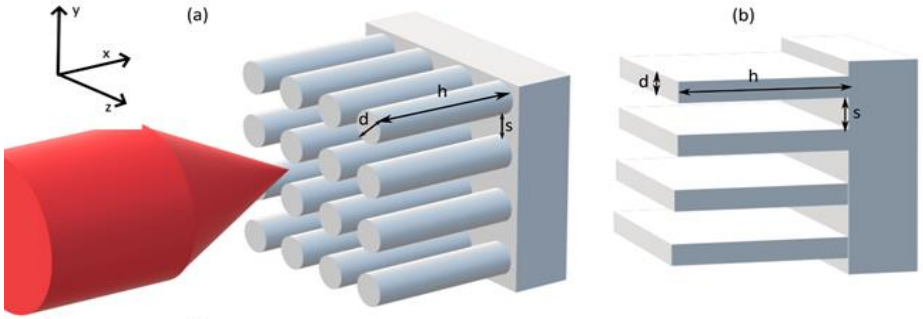

nano/microrods

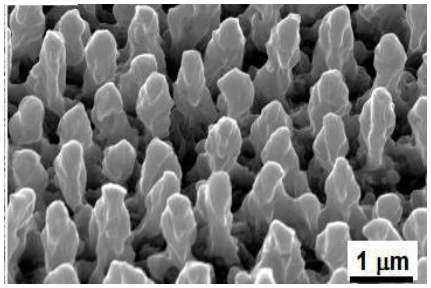

nano/microrelief

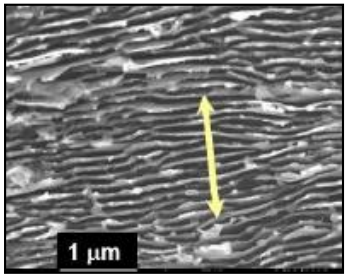

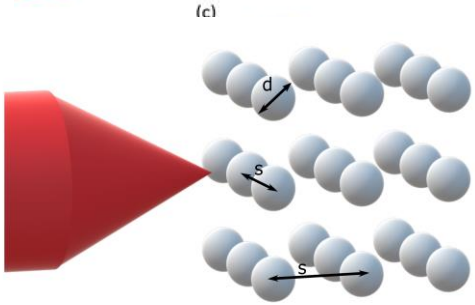

3D PIC simulation optimization of laser-plasma interaction through geometrical matching (d, h, s)

super-ponderomotive electrons

Semi-transparent
High average density
Volumetric heating

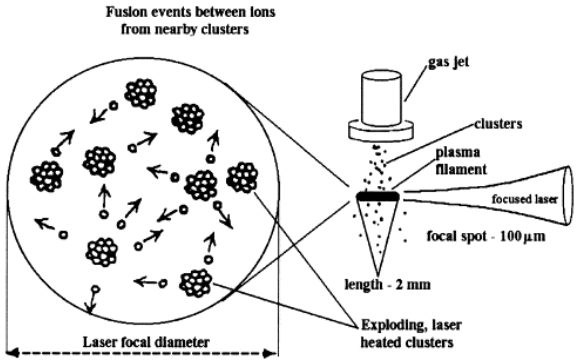

- ❑ **nuclear reactions on a table, neutron source**
- ❑ **secondary e.m. emission**
- ❑ **high energy density research**

Stochastic electron dynamics in complex field

5 mJ, 60 fs laser of 2×10^{18} W/cm^2

D. A. Gozhev *et al.*, HEDP **37**, 100856 (2020)

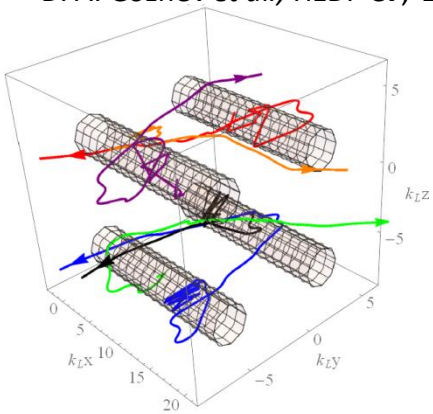

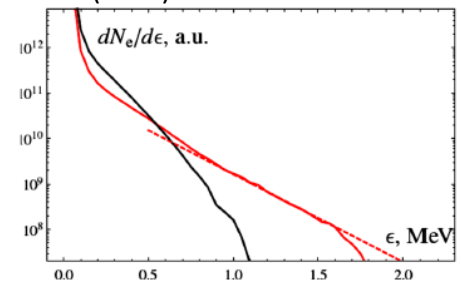

Fig. 4. (a) Hot-electron temperature (shown in blue) and normalized electric field maximum (red) as a function of the interspatial distance (s) for set I of laser parameters, $h/\lambda_L = 1.5$, and $d/\lambda_L = 0.3$. (b) Electron energy spectra for $s = 0.3$ (black), $s = 0.8$ (red) and corresponding exponential fit (dashed red curve). (For interpretation of the references to colour in this figure legend, the reader is referred to the web version of this article.)

NEUTRON PRODUCTION FROM STRUCTURED TARGETS IRRADIATED BY AN ULTRASHORT LASER PULSE,
S. G. Bochkarev *et al.*, JRLR 42, N4 (2021)

25 mJ, 100 Hz laser, (1) Ti + 40% D or (2) 20% D and 20% T
1 : ~ 5×10^7 n°/s (DD) ; 2 : ~ 10^9 n°/s (DT)

Electron acceleration from Au submicron clusters

Laser pulse:
Linear polarized, Plane wave
$\lambda_L = 1\ \mu m$
$\tau_{FWHM} = 10$ fs

$$I_L = 2\times10^{18} - 3.4\times10^{19}\frac{W}{cm^2} \Rightarrow$$

$$a_L = 0.85\sqrt{I{\lambda_L}^2/I_{18}\lambda_1^2} \approx 1.2 - 5$$

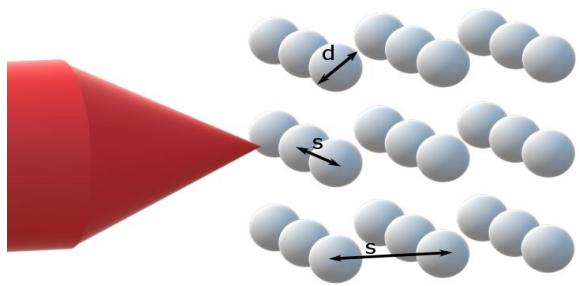

Clusters electron density: $200\ n_{cr}$
Diameter of clusters (d): $0.2\lambda_L$
Average distance between cluster centers (s): $1.2\lambda_L$
Average electron densiry: $0.48\ n_{cr}$

Simulation setup:

Simulation box : $4.5\lambda_L \times 4.5\lambda_L \times 4.5\lambda_L$
Time step: 0.0047 fs
Spatial step : $\frac{\lambda_L}{600} \times \frac{\lambda_L}{200} \times \frac{\lambda_L}{200}$
Particles in cells : 8
Duration of simulation: 60 fs

Boundary conditions:
longitudinal - absorbing
transverse - periodic

Electron distribution in a cluster plasma

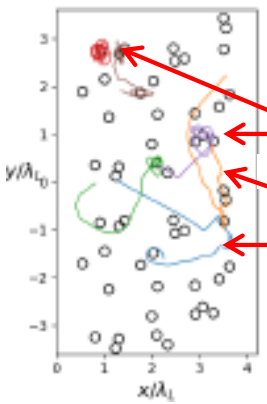

Large angle scattering

Captured electrons, Kepler's orbits

Scattering with hopping

PIC simulations

$I = 2\times10^{18}$ W/cm^2,

$\tau = 30$ fs

Plateau type spectra

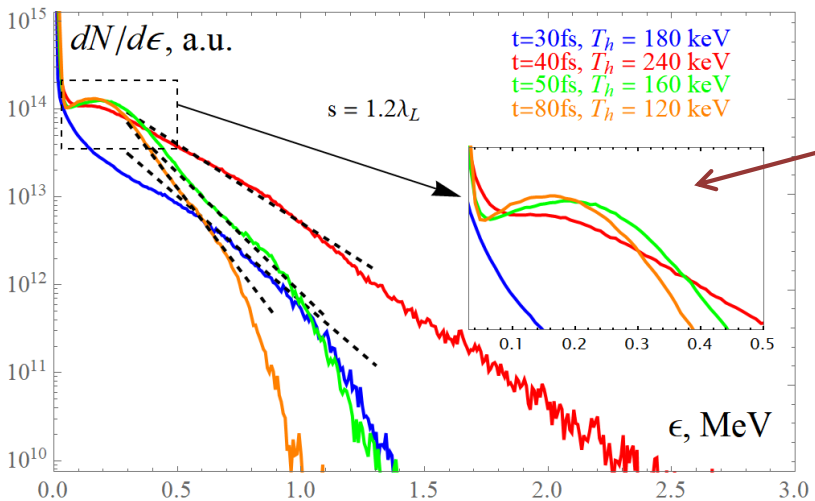

Increased number of high-energy electrons

X-ray cluster source

Recirculating electrons from ultrathin foil

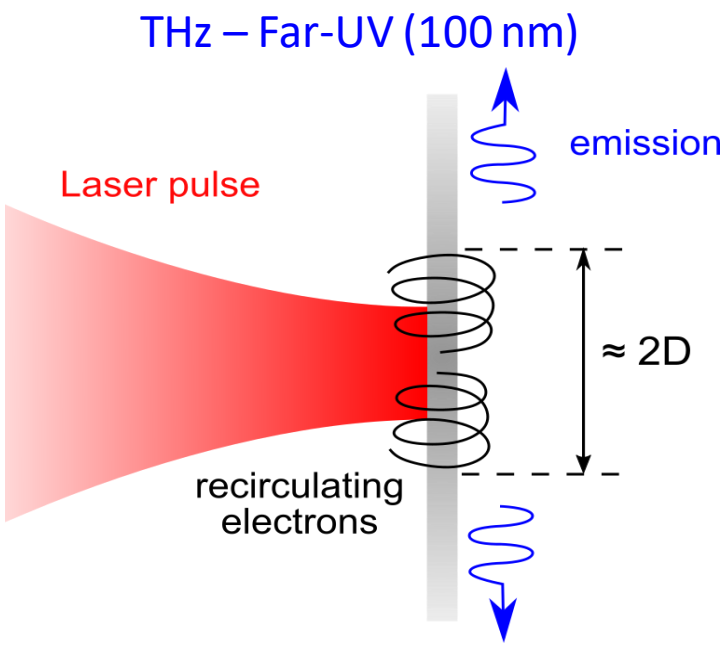

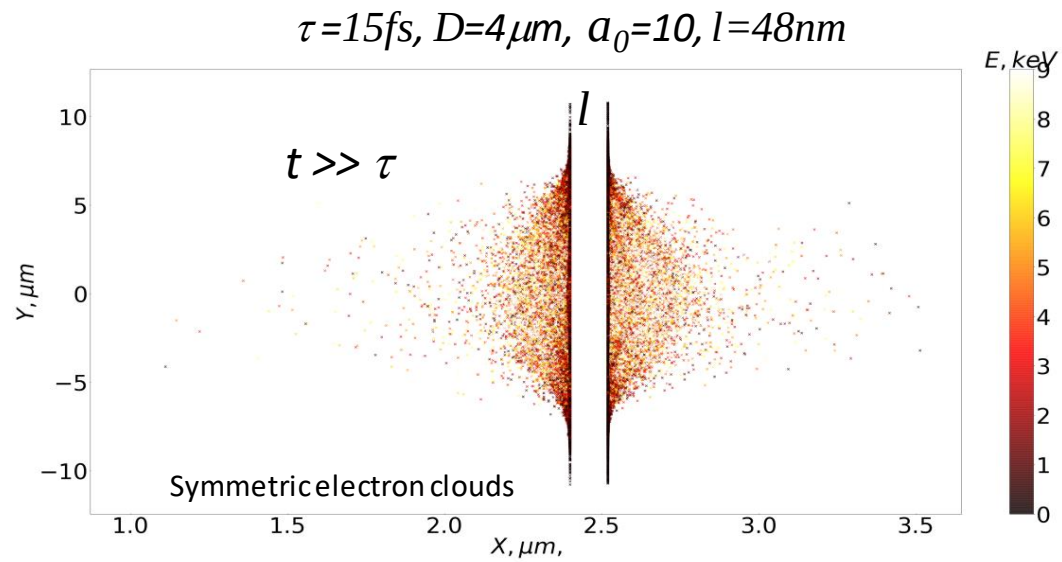

phase plane

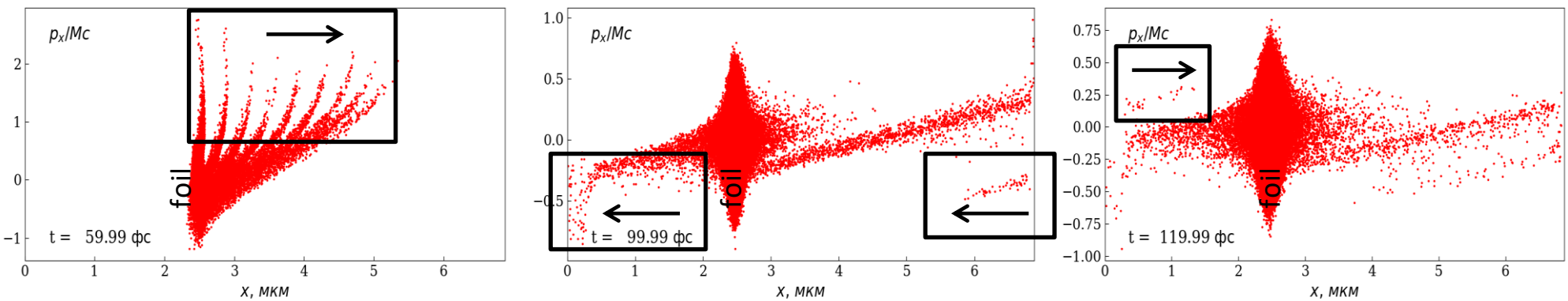

Laser proton acceleration for laser intensity measurement

In collaboration with CUOS UoM, USA (A.M. Maksimchuk, A.G.R. Thomas, K. Krushelnick)

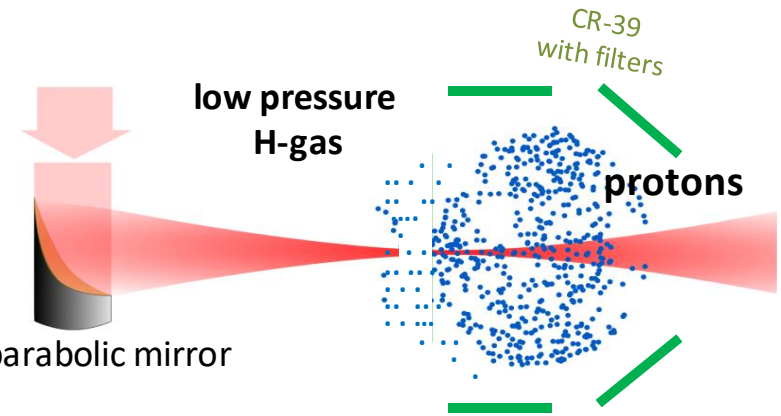

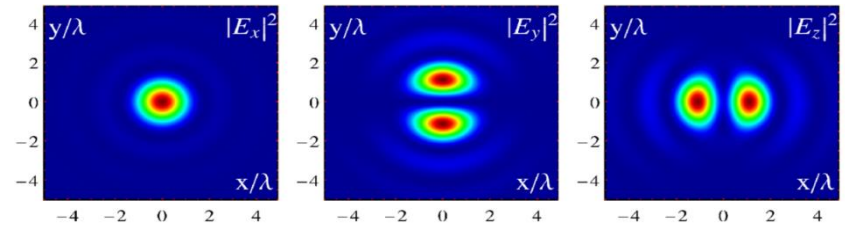

Focusing in diffraction limit

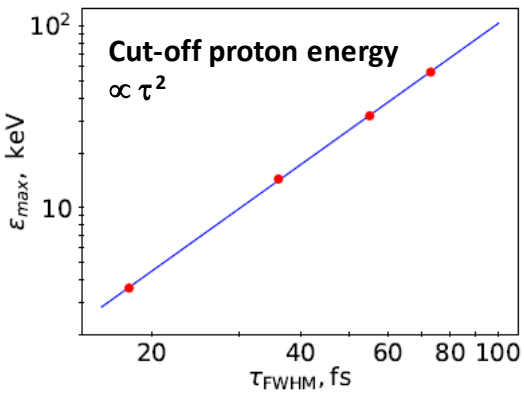

Cut-off energy vs pulse duration. $I=10^{22}$W/cm^2, $D_F = 1.32\lambda$.

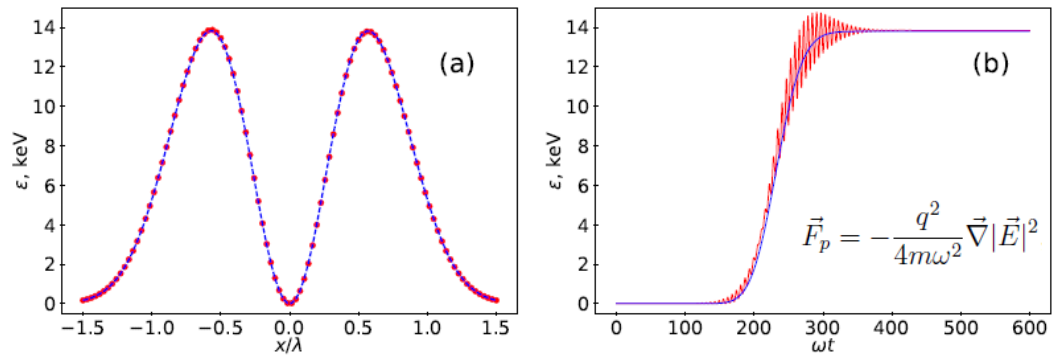

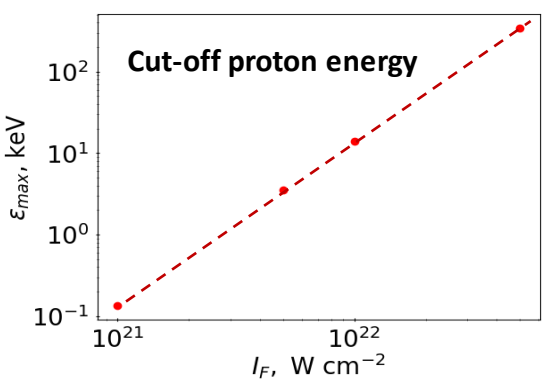

1) O.E.Vais et al., New J. Phys. **22**, 023003 (2020)

2) O.E.Vais et al., PPCF **63**, 014002 (2021)

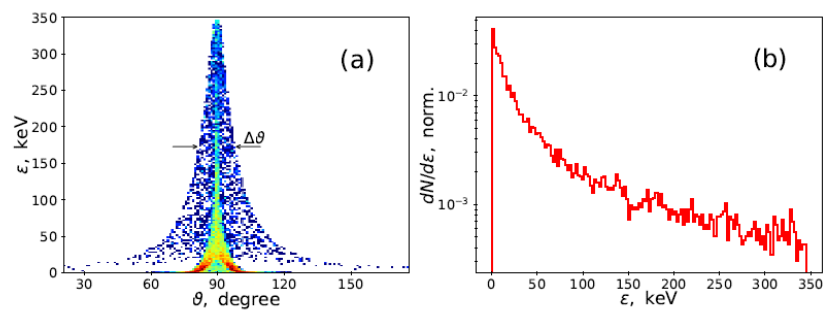

Fig. 3: φ-integrated (a) and angular-integrated (b) spectral distributions of protons accelerated by Gaussian laser pulse with duration $\tau_{FWHM} = 36$fs and peak intensity $I_p = 5\times10^{22}$ W cm^{-2}, focused by off-axis parabolic mirror ($\rho = 5.08$cm, $\psi_{off} = 90°$) into the focal spot $D_F = 1.3\lambda$.

Complementary diagnostics with electrons


Thank you